A mutant allele of the long-day flowering promoter NtFT5 unravels the mystery behind the short-day-specific flowering of tobacco cultivar Maryland Mammoth

Lena Grundmann[1§], Marius M. Zimmermann[2§+], Andrea Känel[2], Axel Schwarze[2+], David R. Wiedmann[1+], Jost Muth[3], Richard M. Twyman[4], Dirk Prüfer[1,2] and Gundula A. Noll[1,2*]

[1]Fraunhofer Institute for Molecular Biology and Applied Ecology IME, Schlossplatz 8, 48143 Münster, Germany,

[2]University of Münster (UM), Institute of Plant Biology and Biotechnology, Schlossplatz 8, 48143 Münster, Germany,

[3]Fraunhofer Institute for Molecular Biology and Applied Ecology IME, Forckenbeckstraße 6, 52074 Aachen, Germany, and

[4]TRM Ltd, PO Box 493, Scarborough, YO11 9FJ, United Kingdom

[§]These authors have contributed equally to this work.

[*]For correspondence: Gundula A. Noll; Schlossplatz 8, 48143 Münster; Tel: +492518324843; gnoll@uni-muenster.de

[+]M. Zimmermann, A. Schwarze and D. Wiedmann were affiliated with UM IBBP/Fraunhofer IME at the time the work was completed.

Authors' email addresses:

lena.grundmann@ime.fraunhofer.de; mariuszimmermann@gmx.net; a.kaenel@uni-muenster.de; axel.schwarze@uni-muenster.de; david-wiedmann@t-online.de; jost.muth@ime.fraunhofer.de; richard@twymanrm.com; dpruefer@uni-muenster.de; gundula.noll@ime.fraunhofer.de

running title: NtFT5 mutation and short-day specific flowering in tobacco
Date of submission: 28.06.2022
Date of revision: 30.04.2024
Number of tables: 0
Number of figures: 5
Word count: 5.283 (Introduction 830; Results 2.987; Discussion 1.317; Supplementary data 127, Acknowledgements 22)
Number of Supplementary figures/tables: 7/1

Highlight

The previously unexplained gigantism of Maryland Mammoth tobacco is caused by a truncated major floral activator protein that results in weaker activation and the inability to flower under long-day conditions.

Abstract

Flowering in day-neutral tobacco (*Nicotiana tabacum*) plants requires the photoperiod-dependent expression of members of the FLOWERING LOCUS T (FT)-like clade of phosphatidylethanolamine-binding proteins. FT-like floral activators and inhibitors compete for interaction with FD proteins to shift from vegetative to reproductive growth. In the short-day (SD) cultivar Maryland Mammoth (MM), vegetative growth persists under long-day (LD) conditions, generating unusually tall plants. We found that the major floral inducer under long-days (NtFT5) was expressed in MM and that *NtFT5* overexpression induced flowering in MM plants under LD conditions. However, sequence analysis revealed a 2-bp deletion near the 3′ end of *NtFT5* in MM plants resulting in a frame shift which leads to an altered amino acid sequence and a premature stop codon. We found that the truncated $NtFT5_{MM}$ protein was still able to interact with tobacco FD proteins. However, constitutive overexpression under LD conditions in SD-specific flowering tobacco plants showed that $NtFT5_{MM}$ is a weaker floral inducer than NtFT5. Our data suggest that the truncation does not impair the stability of the $NtFT5_{MM}$ protein but may affect its binding affinity for NtFD1, probably resulting in the weaker expression of target genes. Our results therefore provide a potential explanation for the MM gigantism phenotype first observed more than 100 years ago.

Keywords and Abbreviations: flower development, FLOWERING LOCUS T, Maryland Mammoth, *Nicotiana tabacum*, non-flowering phenotype, PEBP family, photoperiodism

FLOWERING LOCUS T (FT), long-day (LD), Maryland Mammoth (MM), short-day (SD)

Introduction

The transition from vegetative to reproductive development in flowering plants requires a precisely timed response to multiple endogenous and exogenous factors. In many plant species, a certain day length is required for floral induction. This perception of light and dark, and the subsequent adaptation, is known as photoperiodism, and plants can be assigned to one of three groups on this basis: short-day (SD), long-day (LD) and day-neutral. One of the first experiments addressing photoperiodism involved the tobacco (*Nicotiana tabacum*) cultivar Maryland Mammoth (MM), which does not flower under LD conditions and therefore grows unusually tall (Garner and Allard, 1920). Normally, tetraploid *N. tabacum* displays day-neutral flowering behavior. Many theories were

65 proposed to explain the unanticipated obligate SD flowering of MM (including poor nutrition and
66 transplant shock) before experiments confirmed that photoperiodic conditions were responsible for
67 the LD-specific gigantism phenotype (Garner and Allard, 1920).
68 Since these early studies, the regulation of photoperiodic flowering has been investigated in a
69 number of plant species, in many cases revealing that permissive photoperiodic conditions generate
70 a mobile signal (florigen) that mediates the switch from vegetative to reproductive growth (for
71 review, see Wickland and Hanzawa, 2015). It is now accepted that the FLOWERING LOCUS T (FT)-like
72 protein family is a major part of that signal (for review, see Turck *et al.*, 2008). In many plants, FT is
73 produced in the leaves and transported via the phloem to the shoot apical meristem (SAM), where it
74 interacts with the bZIP transcription factor FD to activate the floral transition (Abe *et al.*, 2005; Wigge
75 *et al.*, 2005; Corbesier *et al.*, 2007; Tamaki *et al.*, 2007).
76 FT belongs to the phosphatidylethanolamine-binding protein (PEBP) family of developmental
77 regulators, which are conserved in all eukaryotic organisms (Schoentgen and Jollès, 1995; Bradley *et*
78 *al.*, 1996; Banfield *et al.*, 1998; Karlgren *et al.*, 2011). Whereas FT proteins are generally floral
79 activators, PEBPs from the TERMINAL FLOWER1 (TFL1)-like clade are floral inhibitors that maintain
80 the inflorescence meristem (Bradley *et al.*, 1996; Kobayashi *et al.*, 1999). Interestingly, the *FT* gene
81 family in some plants has undergone expansion and neofunctionalization, with some members
82 evolving into floral inhibitors (Pin *et al.*, 2010; Harig *et al.*, 2012; Wickland and Hanzawa, 2015). For
83 example, two antagonistic FT homologs have been identified in sugar beet (*Beta vulgaris*), where
84 BvFT1 acts as a floral inhibitor by repressing the floral activator *BvFT2* at the transcriptional level (Pin
85 *et al.*, 2010). In day-neutral tomato plants (*Solanum lycopersicum*), flowering is regulated by the
86 expression of four *FT*-like genes encoding the floral inhibitors SlSP5G, SlSP5G2 and SlSP5G3, and the
87 floral activator SlSP3D. The *SlSP3D* gene is expressed similarly under LD and SD conditions, whereas
88 *SlSP5G* is predominantly expressed under LD conditions, and *SlSP5G2* and *SlSP5G3* are predominantly
89 expressed under SD conditions. Flower development in day-neutral tomato is therefore regulated by
90 the differential photoperiodic expression of multiple *FT*-like genes (Molinero-Rosales *et al.*, 2004;
91 Lifschitz *et al.*, 2006; Cao *et al.*, 2015).
92 The tobacco genome also encodes multiple FT homologs, some of which (NtFT1–NtFT3) are floral
93 inhibitors whereas others (NtFT4 and NtFT5) are floral activators (Harig *et al.*, 2012; Beinecke *et al.*,
94 2018; Wang *et al.*, 2018). *NtFT1–NtFT4* are expressed predominantly under SD conditions whereas
95 *NtFT5* is expressed under both SD and LD conditions, and unlike *FT* genes from other species none of
96 the *NtFT* genes show a circadian expression profile (Harig *et al.*, 2012; Beinecke *et al.*, 2018).
97 Silencing the floral activator gene *NtFT5* by RNA interference significantly delayed flowering under LD
98 conditions, whereas knocking out the *NtFT5* gene using CRISPR/Cas9 rendered the mutants
99 completely unable to flower under LD conditions, indicating that NtFT5 is a major floral inducer

100 during long days (Beinecke *et al.*, 2018; Schmidt *et al.*, 2020). Three functional FD homologs have also
101 been identified in tobacco (NtFD1, NtFD3 and NtFD4) and they interact with tobacco FT proteins
102 (Beinecke *et al.*, 2018). Furthermore, the *NtFT4* and *NtFT2* genes (encoding an activator and
103 inhibitor, respectively) are expressed at similar levels under SD conditions, and the proteins show
104 dose-dependent effects on flowering, which indicates they compete at the protein level for FD
105 binding rather than using the mutual transcriptional regulation strategy described in sugar beet and
106 potato (Pin *et al.*, 2010; Abelenda *et al.*, 2016; Beinecke *et al.*, 2018). Indeed, NtFD1 preferentially
107 interacts with the floral activator NtFT4 rather than the inhibitor NtFT2 (Beinecke *et al.*, 2018). Taken
108 together, these results show that although tobacco is a day-neutral plant, flowering is in part
109 regulated by the photoperiod-dependent expression of different *FT* genes (Harig *et al.*, 2012;
110 Beinecke *et al.*, 2018).
111 Here, we isolated and characterized the *NtFT5* gene in the SD cultivar MM and carried out
112 overexpression studies to investigate its impact on flowering in MM compared to the day-neutral
113 cultivar Hicks, which is considered to be isogenic to MM except at the MM locus (Smith and
114 McDaniel, 1992). Our results provide insight into the molecular basis of a phenomenon that has been
115 observed but not understood for more than a century (Amasino, 2013).

116 **Materials and Methods**

117 **Plant materials and cultivation conditions**

118 Seeds of *N. tabacum* cv. Hicks, *N. tabacum* cv. Maryland Mammoth (IPK Gatersleben, Germany) and
119 *N. tabacum* SR1Δ*NtFT5* were sown in soil and cultivated in the greenhouse under LD conditions (16-h
120 photoperiod, artificial light switched on if natural light fell below 700 µmol m^{-2} s^{-1}, 22–25 °C under
121 light, 20–25 °C in the dark) or in phytotrons under SD conditions (8-h photoperiod, 200 µmol m^{-2} s^{-1},
122 25 °C under light, 22 °C in the dark). Medial leaves were harvested 6 and 10 weeks after seed sowing
123 (WASS) under LD and SD conditions and each sample comprised tissue pooled from three plants.
124 Transgenic tobacco plants were generated by leaf disc transformation (Horsch *et al.*, 1985) using
125 *Agrobacterium tumefaciens* strain LBA4404 (Hoekema *et al.*, 1983) and were regenerated on MS
126 medium (Murashige and Skoog, 1962) containing 25 mg/L hygromycin for sterile selection under LD
127 conditions (100 µmol m^{-2} s^{-1}, 23 °C). After root formation, independent transgenic lines were
128 transferred to the greenhouse and grown in soil. T_1 seedlings were cultivated under sterile conditions
129 on selective medium as above. Seedlings were either harvested for expression and western blot
130 analysis or up to 10 individuals were transferred to the greenhouse for phenotypic analysis.

131 **Gene expression studies**

132 Leaf or seedling samples were snap frozen in liquid nitrogen and stored at –80°C. Total RNA was
133 extracted using the innuPREP Plant RNA kit (Analytik Jena, Jena, Germany) and residual genomic DNA

134 was removed using the Turbo DNA-free kit (Thermo Fisher Scientific, Waltham, MA, USA). First-
135 strand cDNA was synthesized by reverse transcription using PrimeScript RT Master Mix (Takara Bio
136 Group, Saint-Germain-en-Laye, France). We carried out qPCR analysis using the CFX 96 Real-Time
137 system (Bio-Rad, Munich, Germany) on a C1000 Touch Thermal Cycler. We mixed 0.1 µl template
138 cDNA and 500 nM of each primer (Supplementary Table S1) with KAPA SYBR Fast qPCR Master Mix
139 (Merck, Darmstadt, Germany). Each reaction comprised an initial denaturation step for 3 min at 95
140 °C, followed by 40 cycles of denaturation at 95 °C for 3 s and annealing/extension at primer-specific
141 temperatures for 30 s (Supplementary Table S1). Melt curve analysis was carried out to confirm the
142 specificity of the amplicon (5 s, 58–95 °C, ΔT = 0.5 °C). The target transcripts and reference *NtEF-1α*
143 (Schmidt and Delaney, 2010) were analyzed in triplicate, and the quantification cycle (C_q) values of
144 technical replicates were averaged. The NTC (non-template control) and NRT (non-reverse-
145 transcribed control) were analyzed in duplicate. Data were analyzed using Bio-Rad CFX Manager v3.1.
146 The expression values of *NtFT4* and *NtFT5* were determined as previously described (Livak and
147 Schmittgen, 2001).

148 **Cloning experiments**

149 The *NtFT5* and *AtFT* coding sequences were amplified from tobacco cDNA (*N. tabacum* cv. Hicks and
150 cv. MM) and *Arabidopsis thaliana* cDNA (cv. Col-0), respectively, using the primers listed in
151 Supplementary Table S1. The overexpression constructs were prepared by digesting the *NtFT5* and
152 $NtFT5_{MM}$ amplicons with the appropriate restriction enzymes and inserting them into vector pRT104
153 containing the CaMV 35S promoter and terminator (Töpfer *et al.*, 1987). The entire expression
154 cassette was then excised with HindIII and ligated into vector pBinHyg (Bevan, 1984). The expression
155 constructs of *NtFT5* and $NtFT5_{MM}$ under control of the endogenous P-$NtFT5_{2.6kb}$ were prepared by
156 digesting the P-$NtFT5_{2.6kb}$, *NtFT5* and $NtFT5_{MM}$ amplicons with the appropriate restriction enzymes
157 and inserting them into vector plab12.1 containing the 35S terminator (linearized with XmaI/XbaI).
158 For the bimolecular fluorescence complementation (BiFC) assay, the *AtFT, NtFT5* and $NtFT5_{MM}$ coding
159 sequences were amplified using the primers listed in Supplementary Table S1, digested with the
160 appropriate restriction enzymes and inserted into vector pENTR4 (Invitrogen, Karlsruhe, Germany).
161 The pENTR4 constructs were then transferred to pBatTL NmRFP-*ccd*B by LR recombination using the
162 Gateway LR Clonase Enzyme mix (Invitrogen). Split mRFP destination vectors containing *NtFD1*,
163 *NtFD3, NtFD4* and $NtFD1_{SAAPF}$ were already available (Beinecke *et al.*, 2018). Destination vectors were
164 kindly provided by Dr Guido Jach and Dr Joachim Uhrig, MPI Cologne, Germany (Müller *et al.*, 2010).
165 For the multicolor BiFC (mcBiFC) assay, vectors P35S:SCN-NtFT2:Tnos-Spacer and P35S:VN-
166 NtFT2:Tnos pBluescriptII (Beinecke et al., 2018) were digested with StuI/BsrGI and ligated with the
167 *NtFT5* and $NtFT5_{MM}$ coding sequences to generate vectors pBS-*SCN-NtFT5*-Sp, pBS-*SCN-*$NtFT5_{MM}$-Sp,

168 pBS-*VN-NtFT5* and pBS-*VN-NtFT5*$_{MM}$. To generate dual expression cassettes, P35S:*VN-NtFT5*$_{(MM)}$ was
169 excised with ClaI/DraIII and transferred to pBS-*SCN-NtFT5*$_{(MM)}$-Sp to create four intermediate vectors.
170 The dual expression cassettes were excised using PmeI/BamHI and transferred to plab12.1 (linearized
171 with XmnI/BamHI) to create four binary vectors named plab-*SCN-NtFTx*-Sp-*VN-NtFTx*. To generate
172 the SCC-NtFD1 fusion, SCC-HA was amplified using the primers listed in Supplementary Table S1,
173 digested with SalI/BamHI and transferred to pRT104 (linearized with XhoI/BamHI). The NtFD1 coding
174 sequence was amplified, digested with BamHI/XbaI and transferred to pRT-SCC-HA (linearized with
175 BamHI/XbaI). The P35S:SCC-NtFD1:T35S cassette was excised with HindIII and transferred to plab12.1
176 to create the binary vector plab-SCC-NtFD1.
177 The overexpression constructs for *NtFT5*$_{G170W}$ and *NtFT5*$_{MM\ W170G}$ were prepared by digesting the
178 *NtFT5*$_{G170W}$ and *NtFT5*$_{MM\ W170G}$ amplicons (generated using the primers listed in Supplementary Table
179 S1) with the appropriate restriction enzymes and inserting them into vector pRT104, containing the
180 CaMV 35S promoter and terminator (Töpfer *et al.*, 1987). The entire expression cassette was then
181 excised with HindIII and transferred to vector plab12.10 (Post *et al.*, 2014).
182 All constructs for transient and stable expression were introduced into the appropriate strain of
183 *A. tumefaciens* by electroporation.

184 **Fragment length analysis**

185 F_1 and F_2 individuals of the reciprocal cross of Hicks and MM were genotyped by fragment length
186 analysis of the NtFT5 genomic sequence. This was carried out with a fragment of exon 4, containing
187 the NtFT5$_{MM}$-specific 2 bp deletion. The fragment was amplified using primers (see Supplementary
188 Table S1) carrying the fluorescent dye 6-carboxyfluorescein (6-FAM). To identify NtFT5 and NtFT5$_{MM}$
189 alleles the amplicon length of the NtFT5 allele from the cultivar Hicks and of the NtFT5$_{MM}$ allele from
190 the cultivar MM was simultaneously determined and used as references. The PCR samples were
191 mixed with the GeneScan 600 LIZ dye Size Standard v2.0 (Thermo Fisher Scientific) and analyzed in an
192 ABI 3730 Genetic Analyzer (Applied Biosystems, Waltham, MA, USA). The data were evaluated using
193 the Applied Biosystems® Sizing Analysis Module Peak Scanner Software (version 3.0).

194 **Western blotting**

195 Total protein extracted from 3-week-old transgenic and wild-type seedlings was boiled with Laemmli
196 buffer (50% glycerol, 10% SDS, 0.25 M Tris-HCl pH 6.8, 5% 2-mercaptoethanol) containing 0.05%
197 bromophenol blue and was separated by SDS-PAGE on a 12% polyacrylamide gel before
198 electroblotting onto a nylon membrane. NtFT5 protein was detected using an anti-FT antibody
199 (AS06198, Agrisera) diluted 1:1000.

200 **Grafting experiments**

201 SR1 wild-type and 35S:*NtFT5*$_{(MM)}$//SR1Δ*NtFT5* transgenic plants were cultivated in the greenhouse
202 until floral buds became visible. Non-flowering SR1Δ*NtFT5* scions were then grafted onto each stock
203 (n = 3) before further cultivation in the greenhouse. Emerging leaves of the SR1Δ*NtFT5* scions were
204 removed regularly to enhance the source-sink gradient. To ensure seed production of
205 P-NtFT5$_{2.6kb}$:*NtFT5*//SR1Δ*NtFT5* and P-NtFT5$_{2.6kb}$:*NtFT5*$_{MM}$// SR1Δ*NtFT5* scions of these primary
206 transformants were grafted onto florally induced SR1 wild-type plants.

207 **(Multicolor) bimolecular fluorescence complementation analysis**

208 Transient expression was carried out by co-infiltrating the leaves of 3–4-week-old *N. benthamiana*
209 plants (grown under LD conditions) with *A. tumefaciens* strain GV3101 pMP90 carrying the
210 appropriate expression constructs for FT (*AtFT*, *NtFT5*, *NtFT5*$_{MM}$, *NtFT5*$_{FN*}$, *NtFT5*$_{FNC*}$, *NtFT5*$_{R61G}$ or
211 *NtFT5*$_{R129A}$) and FD (*NtFD1*, *NtFD1*$_{SAAPF}$, *NtFD3* or *NtFD4*) and *A. tumefaciens* strain C58C1 carrying the
212 pCH32 helper plasmid encoding virulence genes and the pBIN61 plasmid encoding the tomato bushy
213 stunt virus RNA silencing suppressor protein p19 (Hamilton *et al.*, 1996; Walter *et al.*, 2004). The
214 expression and helper strains were infiltrated at OD_{600nm} 1 and 0.3, respectively. We monitored mRFP
215 fluorescence by confocal laser scanning microscopy (CLSM) using a TCS SP5 X microscope (Leica
216 Microsystems, Wetzlar, Germany) at excitation and emission wavelengths of 549 and 569–629 nm,
217 respectively. For mcBiFC (Hu and Kerppola, 2003; Waadt et al., 2008), the SCN/VN expression strains,
218 the SCC-NtFD1 expression strain and the helper strain were infiltrated at OD_{600nm} = 0.5, 0.33 and 0.3,
219 respectively. Plants were cultivated under continuous light for 3–4 days, and leaf discs were screened
220 for fluorescent cells in the abaxial epidermis. Fluorescence was observed by CLSM using a Leica
221 STELLARIS 8 microscope (Leica Microsystems) at excitation/emission wavelengths of 458/470–490
222 nm for S(CFP) 3A and 488/505–525 nm for the VN/SCC chimera. Nuclear fluorescence was quantified
223 using Leica LAS AF software and the data were analyzed using Origin 2020.

224 **Results**

225 **Expression of endogenous floral activator genes *NtFT4* and *NtFT5* in SD cultivar MM and day-**
226 **neutral cultivar Hicks**

227 Flower development is induced under both LD and SD conditions in most tobacco cultivars, but
228 cultivar MM flowers only under SD conditions (Fig. 1A–H). To determine whether the LD-specific
229 non-flowering phenotype of MM reflects the silencing of *NtFT5*, the major floral activator under LD
230 conditions (Harig *et al.*, 2012; Beinecke *et al.*, 2018; Schmidt et al., 2020), we compared the
231 expression of *NtFT5* in MM and a day-neutral tobacco cultivar (Hicks) by quantitative real-time PCR
232 (qPCR) (Fig. 1I–J). We found that *NtFT5* was expressed in both cultivars under LD and SD conditions
233 and the expression profiles were similar in each cultivar when matched for day length and the time
234 point of harvest (6 or 10 WASS). *NtFT5* mRNA was generally less abundant under LD than SD

235 conditions in both cultivars, and under SD conditions *NtFT5* was expressed at basal levels 6 WASS but
236 was induced during floral transition (10 WASS). The main difference between the cultivars was that
237 *NtFT5* mRNA levels were higher in Hicks than MM under LD conditions at the 6 WASS time point.
238 However, *NtFT5* mRNA levels increased between 6 and 10 WASS under LD conditions in MM whereas
239 we detected almost no difference in *NtFT5* mRNA levels between 6 and 10 WASS under LD conditions
240 in Hicks. The increase in *NtFT5* mRNA levels between 6 and 10 WASS was less steep in MM under LD
241 conditions than SD conditions. *NtFT5* mRNA levels were nearly identical in both cultivars 10 WASS
242 under LD conditions, but Hicks flowered at this point whereas MM remained in the vegetative phase.
243 In addition to *NtFT5* the closely related gene *NtFT7* was identified in whole-genome shotgun contigs
244 of the *N. tabacum* cultivars K326, TN90 and Basma Xanthi, and it promoted the flowering of *N.*
245 *sylvestris* plants constitutively overexpressing this gene (Beinecke *et al.*, 2018). However, as
246 previously described for cultivar SR1 (Beinecke *et al.*, 2018), *NtFT7* was not detected in the genomes
247 of cultivars Hicks or MM (Supplementary Fig. S1). We also analyzed the expression of *NtFT4*, which
248 encodes a floral activator that is predominantly expressed under SD conditions in cultivar SR1 (Harig
249 *et al.*, 2012; Beinecke *et al.*, 2018). Our qPCR results showed that *NtFT4* was also predominantly
250 expressed under SD conditions in cultivars Hicks and MM, and the mRNA levels increased during the
251 reproductive phase. *NtFT4* mRNA was also detected under LD conditions, mainly at 10 WASS, and the
252 levels were comparable to those detected under SD conditions 6 WASS (Fig. 1I–J). Interestingly,
253 flowering was delayed by a week in MM compared to Hicks under SD conditions, even though *NtFT4*
254 and *NtFT5* were expressed at similar levels in both cultivars.

255 **Floral induction in transgenic MM and Hicks plants expressing *NtFT5***

256 Having established that *NtFT5* is similarly expressed in both cultivars, we set out to determine
257 whether there is a functional deficiency in the *NtFT5* gene in MM and whether MM has the
258 propensity to flower under LD conditions when provided with a fully functional sequence. We
259 therefore isolated the *NtFT5* coding sequence from Hicks (because this variety flowers under LD
260 conditions) and transformed MM plants (and Hicks plants as a control) with the 35S:$NtFT5_{Hicks}$
261 cassette. The constitutive expression of the $NtFT5_{Hicks}$ gene caused a profound early flowering
262 phenotype in both cultivars (Fig. 2A,B). We found that 50% of the lines began flowering in tissue
263 culture and failed to form roots (four 35S:$NtFT5_{Hicks}$ MM lines and five 35S:$NtFT5_{Hicks}$ Hicks lines), but
264 the other 50% could be transferred to the greenhouse and generated seeds. Expression analysis by
265 qPCR revealed that transgenic lines from both cultivars accumulated ~10^4-fold more *NtFT5* mRNA
266 than the vector control (Fig. 2C,D). For a more detailed analysis, we studied the T_1 progeny of two
267 independent transgenic lines and one vector control line for each cultivar in the greenhouse under
268 LD conditions (Fig. 2E,F). We observed a profound early flowering phenotype for all transgenic lines

269 overexpressing *NtFT5*$_{Hicks}$ resulting in significantly fewer leaves and significantly fewer days until
270 flowering compared to the Hicks and non-flowering MM vector control lines. These results
271 demonstrate that the *NtFT5*$_{Hicks}$ gene can induce flowering during the early stages of development
272 even under LD conditions when overexpressed in the SD cultivar MM.

273 **Functional characterization of NtFT5$_{MM}$**

274 The experiments described above showed that *NtFT5* expression is not suppressed in cultivar MM
275 but that there appears to be a functional difference between the *NtFT5* genes in each cultivar. We
276 therefore compared the *NtFT5*$_{Hicks}$ and *NtFT5*$_{MM}$ coding sequences. This revealed that the *NtFT5*$_{Hicks}$
277 coding sequence was identical to that previously reported for cultivar SR1 (Beinecke *et al.*, 2018). We
278 therefore use the generic designation *NtFT5* hereafter when referring to the *NtFT5*$_{Hicks}$ gene and
279 corresponding protein. In contrast, the *NtFT5*$_{MM}$ sequence featured a 2-bp deletion 29 bp upstream
280 of the stop codon. The resulting frameshift mutation altered the remainder of the amino acid
281 sequence and introduced a premature stop codon, shortening the protein sequence by six amino
282 acids (Fig. 3A).

283 We next attempted to confirm the ability of NtFT5$_{MM}$ to act as a floral promoter. We previously
284 generated *NtFT5*-deficient SR1 plants (SR1Δ*NtFT5*) using the CRISPR/Cas9 system and they were
285 unable to flower under LD conditions (Schmidt *et al.*, 2020). We therefore transformed these
286 SR1Δ*NtFT5* plants with constructs expressing *NtFT5* or *NtFT5*$_{MM}$ under the control of the constitutive
287 CaMV 35S promoter (Fig. 3B–D). Ten out of 13 35S:*NtFT5* transgenic plants showed a profound early
288 flowering phenotype that failed to produce roots and thus could not be transferred to the
289 greenhouse for the generation of seeds. In contrast, none of the 12 35S:*NtFT5*$_{MM}$ transgenic plants
290 flowered in tissue culture but when transferred to the greenhouse after root induction they started
291 flowering at a later developmental stage (Fig. 3B). We analyzed transgene expression in young leaf
292 tissue by qPCR (the primers amplified the same 190-bp fragment in the coding sequence of *NtFT5*
293 and *NtFT5*$_{MM}$) and detected higher *NtFT5*$_{MM}$ and *NtFT5* mRNA levels in the transgenic plants than in
294 the SR1 vector control (Fig. 3D). Floral induction by *NtFT5*$_{MM}$ was investigated in more detail by
295 studying these transgenic *N. tabacum* cv. SR1Δ*NtFT5* lines in the T_1 generation (Fig. 3E–H). We
296 cultivated three independent transgenic lines each (n = 8–10) and one SR1 vector control line (n = 10)
297 in the greenhouse under LD conditions and documented the late and early flowering phenotype for
298 one representative transgenic line each in comparison to a vector control (Fig. 3E). Although *NtFT5*$_{MM}$
299 mRNA levels strongly increased compared to transgenic plants overexpressing *NtFT5* and the vector
300 control (Fig. 3F), *NtFT5*$_{MM}$ overexpression did not induce early flowering in the SR1Δ*NtFT5* plants as
301 already observed with primary transformants. Moreover, flowering was significantly delayed in all
302 three 35S:*NtFT5*$_{MM}$//SR1Δ*NtFT5* lines and the number of leaves increased significantly compared to

303 the SR1 vector control (Fig. 3G,H). In comparison, all individuals of the three transgenic lines
304 overexpressing *NtFT5* showed a profound early flowering phenotype, resulting in significantly fewer
305 leaves and significantly fewer days until flowering compared to the SR1 vector control with
306 endogenous *NtFT5* expression (Fig. 3G,H). This indicates that $NtFT5_{MM}$ only partially complements the
307 non-flowering phenotype of SR1Δ*NtFT5* plants, showing that $NtFT5_{MM}$ is a weaker floral inducer than
308 NtFT5.
309 We also transformed SR1Δ*NtFT5* and MM plants with constructs expressing *NtFT5* or $NtFT5_{MM}$ under
310 the control of the endogenous NtFT5 promoter (~2.6kb; Supplementary Fig. S2A,B). None of these
311 primary P-$NtFT5_{2.6kb}$:*NtFT5* and P-$NtFT5_{2.6kb}$:$NtFT5_{MM}$ transgenic plants flowered in tissue culture or
312 after transfer to the greenhouse (LD conditions). To overcome the non-flowering phenotype and
313 facilitate seed production, these plants were grafted onto florally induced wild-type SR1 rootstocks.
314 Following successful germination on selective media, we cultivated at least two independent
315 transgenic lines per construct (n=10), one MM vector control line and MM wild-type plants (n = 5) in
316 the greenhouse under LD conditions and documented, if the non-flowering phenotype of SR1Δ*NtFT5*
317 and MM transgenic plants is complemented by these constructs. In the SR1Δ*NtFT5* background, 9–10
318 transgenic plants per line expressing P-$NtFT5_{2.6kb}$:*NtFT5* started flowering while none of the
319 transgenic plants expressing P-$NtFT5_{2.6kb}$:$NtFT5_{MM}$ in SR1Δ*NtFT5* background starting flowering
320 (Supplementary Fig. S2A,C). When expressing *NtFT5* under the control of the endogenous NtFT5
321 promoter in the MM background, plants from four out of six analyzed lines started flowering in the
322 T_1-generation. Here, out of 10 transgenic plants, three (L5), four (L1, L8) and seven (L7) flowered
323 within the experimental time frame (Supplementary Fig. S2B,C). In contrast, when expressing
324 $NtFT5_{MM}$ under the control of the endogenous NtFT5 promoter in the MM background, none of the
325 seventy analyzed plants (10 plants for each of the seven analyzed lines) flowered (Supplementary Fig.
326 S2B,C).
327 Thus, only expression of *NtFT5* but not $NtFT5_{MM}$ under control of its own promoter could partially
328 complement the non-flowering phenotype of SR1Δ*NtFT5* and MM plants, showing again that
329 $NtFT5_{MM}$ is a weaker floral inducer than NtFT5. However, as not all P-$NtFT5_{2.6kb}$:*NtFT5*//MM plants
330 flowered the expression of *NtFT5* under control of the 2.6kb endogenous promoter fragment does
331 not fully resemble the native *NtFT5* expression.
332 We further examined if the homozygous, 2-bp deletion detected in $NtFT5_{MM}$ in the cultivar MM
333 correlates with a non-flowering phenotype after introgression of a functional NtFT5 allele by crossing
334 the cultivar MM with the cultivar Hicks (Fig. 4A). We therefore grew plants of both cultivars under SD
335 conditions to induce flowering and performed reciprocal crossings of the two cultivars. F_1-seeds for
336 each reciprocal cross were sown in soil and ten plants each were grown in the greenhouse under LD
337 conditions. All plants flowered and we genotyped the plants by fragment length analysis (FLA)

338 thereby detecting one *NtFT5* and one *NtFT5*$_{MM}$ allele from each parental cultivar as expected. We
339 then pooled the seeds of 10 F_1 plants for each reciprocal cross and cultivated 95 F_2 plants each
340 together with the parental cultivars (n=9-10) in the greenhouse under LD. We documented the days
341 until flowering and leaf number when the first flower had opened and genotyped each plant for the
342 presence of the NtFT5 and NtFT5$_{MM}$ alleles (Fig. 4 B,C; Supplementary Table S2). All plants of cultivar
343 Hicks started flowering after 46 days with a mean number of 20 leaves, while none of the MM plants
344 started flowering until the end of the experiment after 120 days. In this timeframe, we observed 155
345 flowering and 35 non-flowering F_2 plants. Genotyping the F_2 plants revealed that all non-flowering F_2
346 plants carried the NtFT5$_{MM}$ allele, 112 flowering F_2 plants had one allele of each parental cultivar
347 (NtFT5/NtFT5$_{MM}$) and 43 flowering F_2 plants carried only the NtFT5 allele. Interestingly, F_2 plants with
348 two functional NtFT5 alleles flowered on average after 52 days with a mean number of 22.5 leaves,
349 while F_2 plants with heterozygous NtFT5/NtFT5$_{MM}$ alleles flowered on average after 59 days with a
350 mean number of 26 leaves (Fig. 4 B,C). We could therefore show that the non-flowering MM
351 phenotype under LD clearly segregates with the NtFT5$_{MM}$ allele and that the presence of two
352 functional NtFT5 alleles mediates earlier flowering in comparison to plants with only one functional
353 NtFT5 allele.
354 To gain more insight into the mechanistic difference between NtFT5 and NtFT5$_{MM}$, we determined
355 whether the truncated NtFT5$_{MM}$ protein was able to interact with the recently identified tobacco FD
356 proteins (Beinecke *et al.*, 2018). To initiate floral development, FT interacts with FD in the SAM
357 (Kardailsky *et al.*, 1999; Kobayashi *et al.*, 1999; Abe *et al.*, 2005; Wigge *et al.*, 2005) and similar FT/FD
358 interactions have been described in tobacco (Beinecke *et al.*, 2018). We conducted BiFC assays in
359 which the C-terminal portion of the fluorescent reporter protein mRFP was fused to the N-terminus
360 of NtFD1, NtFD3, NtFD4, or NtFD1 with a mutated STAPF motif (negative control NtFD1$_{SAAPF}$), which
361 does not interact with tobacco FTs due to a missing phosphorylation site (Beinecke *et al.*, 2018). The
362 N-terminal portion of mRFP was fused to the N-terminus of NtFT5$_{MM}$, NtFT5, the well-characterized
363 AtFT as a positive control, and a truncated version of NtFT5 lacking 15 amino acids (NtFT5$_{FN}$) as a
364 negative control (Supplementary Method S1). The CmRFP-FD proteins were coexpressed
365 systematically with the NmRFP-FT proteins. As expected, CLSM revealed a nuclear fluorescent signal
366 for AtFT with any of the three native NtFD proteins (Supplementary Fig. S3) but not when NtFT5$_{FN*}$
367 was combined with these native NtFDs (Fig. 5A, Supplementary Fig. S3). Furthermore, nuclear
368 fluorescence was detected when either NtFT5$_{MM}$ or NtFT5 was present with any of the three native
369 NtFD proteins (NtFD1 is shown as a representative example in Fig. 5A, for the others see
370 Supplementary Fig. S3), but not with NtFD1$_{SAAPF}$ (Fig. 5B). We confirmed the presence of the different
371 mRFP-FT fusion proteins by western blot analysis (Supplementary Fig. S4).

372 Next, we determined whether the C-terminal truncation of NtFT5$_{MM}$ affects protein stability. Crude
373 protein extracts of T_1 seedlings from three independent transgenic lines (same lines as in Fig. 3) and
374 SR1 wild-type seedlings as controls were used for western blotting. We detected NtFT5 and NtFT5$_{MM}$
375 using the AtFT-specific antibody only in crude protein extracts of transgenic seedlings overexpressing
376 the corresponding NtFT. Specific signals were present for one 35S:*NtFT5*//SR1Δ*NtFT5* line (L3), as
377 well as two 35S:*NtFT5*$_{MM}$//SR1Δ*NtFT5* lines (L14 and L24, Fig. 5C). The band for NtFT5$_{MM}$ samples
378 migrated further, reflecting its lower molecular weight due to the truncated C-terminus. This
379 experiment demonstrated that the truncated C-terminus of NtFT5$_{MM}$ does not appear to affect
380 protein stability.
381 Next, we investigated whether the truncation of NtFT5$_{MM}$ impairs the transport of this protein via the
382 phloem. We therefore grafted SR1Δ*NtFT5* scions onto rootstocks of either 35S:*NtFT5*//SR1Δ*NtFT5* or
383 35S:*NtFT5*$_{MM}$//SR1Δ*NtFT5* lines as well as wild-type control plants (n = 3 each). All SR1Δ*NtFT5* scions
384 grafted onto wild-type control stocks flowered 7–9 weeks after grafting, with 35–49 leaves/nodes
385 produced on the scion (Fig. 5D). After approximately 11 weeks, one SR1Δ*NtFT5* scion grafted onto
386 35S:*NtFT5*//SR1Δ*NtFT5* stock, and two grafted onto 35S:*NtFT5*$_{MM}$//SR1Δ*NtFT5* stocks, showed floral-
387 like structures, with 21 and 24/25 leaves/nodes produced on the scion, respectively (Fig. 5D).
388 However, only 50% of these grafts showed floral transition of the SAM, and complete inflorescences
389 (as induced by wild-type stocks) were not formed. Given that 35S:*NtFT5*//SR1Δ*NtFT5* stocks
390 produced many axillary shoots (which we removed regularly) this may have impaired source–sink
391 transport to the scion. For the 35S:*NtFT5*$_{MM}$//SR1Δ*NtFT5* stocks, this might indicate a functionally
392 impaired NtFT5$_{MM}$ protein. These results suggest that NtFT5$_{MM}$ is transported to the shoot apex like
393 NtFT5 but floral transition mediated by 35S:*NtFT5*$_{MM}$//SR1Δ*NtFT5* stocks was slightly delayed
394 compared to floral transition of the SR1Δ*NtFT5* scion grafted onto a 35S:*NtFT5*//SR1Δ*NtFT5* stock,
395 again matching our earlier results that NtFT5$_{MM}$ is a weaker floral inducer.
396 Because the transport of NtFT5$_{MM}$ was apparently normal, we conducted mcBiFC assays to test the
397 binding affinity of both NtFTs with NtFD1. Using this assay, we recently confirmed the lower binding
398 affinity of floral repressor NtFT2 to NtFD1 compared to floral activator NtFT4 (Beinecke *et al.*, 2018).
399 We therefore prepared two cassettes controlled by the CaMV 35S promoter for the expression of
400 NtFT5 or NtFT5$_{MM}$ as N-terminal fusions with the N-terminal component of cyan fluorescent protein
401 S(CFP)3A (SCN) together with an N-terminal fusion of NtFT5 or NtFT5$_{MM}$ with the N-terminal
402 component of Venus (VN) (Supplementary Fig. S5). A construct in which the N-terminal portion of
403 NtFD1 was fused to the C-terminal portion of S(CFP)3A (SCC) was carried by a separate bacterial
404 strain. Interactions between SCN and SCC reconstitute S(CFP)3A, which emits blue fluorescence when
405 excited, whereas chimeric association between VN and SCC emits green fluorescence. After
406 agroinfiltration and the cultivation of *N. benthamiana* under constant light for 3 days, abaxial

407 epidermal leaf cells were analyzed by CLSM and the nuclear signal intensity was measured. The co-
408 expression of SCN-NtFT5 and VN-NtFT5 with SCC-NtFD1, as well as SCN-NtFT5$_{MM}$ and VN-NtFT5$_{MM}$
409 with SCC-NtFD1, resulted in little difference between the blue and green signals and served as an
410 equilibrium control with balanced competition (Fig. 5E and Supplementary Fig. S5). However, when
411 SCN-NtFT5, VN-NtFT5$_{MM}$ and SCC-NtFD1 were co-expressed, a significant shift towards the blue signal
412 of SCN/SCC was detected, whereas the co-expression of SCN-NtFT5$_{MM}$, VN-NtFT5 and SCC-NtFD1
413 produced a dominant green VN/SCC signal. This suggests that NtFT5$_{MM}$ may have a lower binding
414 affinity than NtFT5 for NtFD1, and that NtFD1 may preferably associate with NtFT5 because it is more
415 competitive at the protein level than NtFT5$_{MM}$ with its truncated C-terminus.
416 Our results show that the C-terminal amino acid residues of NtFT5 fulfil an important role in floral
417 transition. Arabidopsis mutants with the substitution G171E in the corresponding region have a late
418 flowering phenotype (Koornneef *et al.*, 1991; Kardailsky *et al.*, 1999; Kobayashi *et al.*, 1999). In
419 NtFT5$_{MM}$, a tryptophan residue is present at the corresponding glycine position (G170W) so we
420 designed overexpression constructs with reciprocal amino acid substitutions (namely *NtFT5*$_{G170W}$ and
421 *NtFT5*$_{MM\ W170G}$) and analyzed these in transgenic SR1Δ*NtFT5* lines (Supplementary Fig. S6A). We
422 regenerated three independent 35S:*NtFT5*$_{G170W}$ and 35S:*NtFT5*$_{MM\ W170G}$ transgenic lines each and
423 investigated these lines in the T_1 generation compared to 35S:*NtFT5* and 35S:*NtFT5*$_{MM}$ transgenic
424 lines in more detail (Fig. 5F,G and Supplementary Fig. S6B,C). We cultivated three independent
425 transgenic lines each (n = 6–10) and one SR1 vector control line (n = 10) in the greenhouse under LD
426 conditions and documented the flowering phenotype for one representative transgenic line each in
427 comparison to a vector control (Fig. 5F). The *NtFT5*$_{G170W}$ and *NtFT5*$_{MM\ W170G}$ mRNA levels were much
428 higher than the vector control and were in the range of the *NtFT5*$_{MM}$ mRNA overexpression levels
429 (Supplementary Fig. S6B). However, *NtFT5*$_{MM\ W170G}$//SR1Δ*NtFT5* lines flowered significantly earlier
430 and the number of leaves was significantly lower compared to the 35S:*NtFT5*$_{MM}$//SR1Δ*NtFT5* lines
431 (Fig. 5G and Supplementary Fig. S6C). Accordingly, 35:*NtFT5*$_{G170W}$//SR1Δ*NtFT5* lines flowered later
432 than 35S:*NtFT5*//SR1Δ*NtFT5* overexpressing plants, resulting in the production of significantly more
433 leaves and significantly more days until flowering (Fig. 5G and Supplementary Fig. S6C). This indicates
434 that both substitutions at position 170, tryptophan to glycine (in NtFT5$_{MM\ W170G}$) and glycine to
435 tryptophan (in NtFT5$_{G170W}$), produced intermediate-strength floral inducers stronger than NtFT5$_{MM}$
436 but weaker than NtFT5.

437 **Discussion**

438 Many plant species initiate the developmental switch from vegetative to reproductive growth under
439 specific photoperiodic conditions. Although tobacco is a day-neutral species, floral initiation depends
440 on the photoperiod-dependent expression of various *FT* genes (Harig *et al.*, 2012; Beinecke *et al.*,

441 2018). Previous studies have mostly focused on *FT* genes expressed under SD conditions, but the
442 recently identified *NtFT5* gene is expressed under both SD and LD conditions. NtFT5 has been
443 characterized as the major floral activator under LD conditions in tobacco cultivar SR1, making this
444 protein an interesting candidate for further analysis in the SD cultivar MM (Beinecke *et al.*, 2018;
445 Schmidt *et al.*, 2020).
446 Comparative expression analysis revealed that *NtFT5* is expressed at similar levels in cultivar MM and
447 the day-neutral cultivar Hicks, which excludes the possibility that the LD-specific non-flowering
448 phenotype of MM is caused by the silencing of this locus (Fig. 1I,J). We also found that the *NtFT5*
449 coding sequence was identical in cultivars Hicks and SR1, and that the overexpression of this
450 sequence in MM permitted flowering under LD conditions (Fig. 2), suggesting that the $NtFT5_{MM}$
451 protein may be functionally impaired. Further analysis revealed a 2-bp deletion near the 3′ end of
452 the $NtFT5_{MM}$ gene causing a frameshift that introduced a premature termination codon and an
453 altered C-terminus (Fig. 3A). By analyzing the F_2 offspring of the reciprocal crossings between the
454 cultivars Hicks and MM we showed that this 2-bp deletion in the $NtFT5_{MM}$ gene is tightly linked with a
455 non-flowering phenotype under LD if present homozygously ($NtFT5_{MM}$/ $NtFT5_{MM}$) and confers
456 delayed flowering if present heterozygously ($NtFT5_{MM}$/ *NtFT5*) (Fig. 4). A similar effect was also
457 described for *NtFT5* knockout mutations (Schmidt *et al.*, 2020). The 2-bp deletion near the 3′ end of
458 the $NtFT5_{MM}$ gene results in a $NtFT5_{MM}$ protein that lacks the six amino acids normally found at the
459 C-terminus and exhibits five amino acids substitutions at the C-terminus (Fig. 3A). Because the
460 $NtFT5_{MM}$ protein could be detected by western blot and floral structures at the SAM of SR1Δ*NtFT5*
461 scions grafted onto 35S:$NtFT5_{MM}$//SR1Δ*NtFT5* stocks were induced (Fig. 5C,D), we concluded that
462 neither protein stability nor transport is affected by the C-terminal truncation and alteration of
463 $NtFT5_{MM}$. We tested the ability of NtFT5 and $NtFT5_{MM}$ to induce flowering under LD conditions by
464 expressing each variant in SR1Δ*NtFT5* plants. As expected, *NtFT5* overexpression resulted in a
465 profound early flowering phenotype (Fig. 3B,G,H), as described for transgenic tobacco lines
466 overexpressing other floral activators such as NtFT4 and AtFT (Harig *et al.*, 2012; Beinecke *et al.*,
467 2018). In contrast, the overexpression of $NtFT5_{MM}$ caused plants to flower at a later developmental
468 stage, even though $NtFT5_{MM}$ mRNA levels were higher than *NtFT5* mRNA levels in the corresponding
469 transgenic SR1Δ*NtFT5* plants (Fig. 3C,G,H). The late-flowering behavior of transgenic
470 35S:$NtFT5_{MM}$//SR1Δ*NtFT5* compared with the normal flowering time of SR1 vector control lines
471 (expressing *NtFT5* at the endogenous level) showed that a fully functional endogenous *NtFT5* gene
472 can more effectively induce flowering than the strong overexpression of $NtFT5_{MM}$. In line with, this
473 we could show that only the expression of *NtFT5* under control of its endogenous promoter could
474 complement the non-flowering phenotypes of SR1Δ*NtFT5* and MM plants while expression of

475 P-NtFT5$_{2.6kb}$:*NtFT5*$_{MM}$ did not induce flowering (Supplementary Fig. S2). This suggests that the
476 truncated and altered C-terminus of *NtFT5*$_{MM}$ weakens its function as a floral activator.
477 As previously shown in Arabidopsis and rice, FT proteins interact with FD proteins to regulate flower
478 development (Abe *et al.*, 2005; Wigge *et al.*, 2005; Taoka *et al.*, 2011). Similarly, the tobacco FT
479 proteins interact with three FD proteins, and it was therefore important to determine whether the
480 truncated NtFT5$_{MM}$ protein retained this ability (Beinecke *et al.*, 2018). Our BiFC experiments showed
481 that both NtFT5 and NtFT5$_{MM}$ interacted with all three tobacco FD proteins, but mcBiFC experiments
482 revealed that NtFD1 may preferably associate with NtFT5 because it is more competitive than
483 NtFT5$_{MM}$ at the protein level (Fig. 5A,B,E; Supplementary Fig. S3). It is widely accepted that 14-3-3
484 proteins mediate interactions between FT and FD (Pnueli *et al.*, 2001; Ho and Weigel, 2014; Taoka *et*
485 *al.*, 2011; Collani *et al.*, 2019; Zuo *et al.*, 2021) and the amino acid residues critical for this interaction
486 are highly conserved in FT-like proteins from angiosperms and are located upstream of the 2-bp
487 deletion in *NtFT5*$_{MM}$. However, our results suggest that additional amino acids at the NtFT5
488 C-terminus are required for proper interaction with NtFD proteins. Furthermore, the C-terminal
489 residues of NtFT5 fulfil an important role in floral activation as shown by the late flowering
490 phenotype of AtFT mutants with the substitution G171E (Koornneef *et al.*, 1991; Kardailsky *et al.*,
491 1999; Kobayashi *et al.*, 1999). In NtFT5$_{MM}$, the corresponding glycine residue is replaced with
492 tryptophan (G170W), suggesting that the truncated and altered C-terminus of NtFT5$_{MM}$ may
493 influence its regulatory activity or binding affinity for NtFD1. Indeed, replacing the tryptophan
494 residue in NtFT5$_{MM}$ with glycine in transgenic 35S:*NtFT5*$_{MM\ W170G}$//SR1Δ*NtFT5* lines restored wild-type
495 flowering behavior, whereas mutating the glycine residue to tryptophan in transgenic
496 35S:*NtFT5*$_{G170W}$//SR1Δ*NtFT5* lines abolished the profound early flowering phenotype (Fig. 5F,G).
497 Furthermore, experiments in Arabidopsis have shown that the overexpression of a truncated *FT* gene
498 yielding a protein lacking the last seven amino acids (FTΔ168) causes a late flowering phenotype in *ft-*
499 *10* mutant plants compared to *ft-10* plants overexpressing functional *FT* (Kim *et al.*, 2016). FTΔ168
500 and NtFT5$_{MM}$ both lack the glycine residue at position 170/171, which is strongly conserved in the FT-
501 like family. Interestingly, members of the TFL1-like family of floral repressors have a highly conserved
502 C-terminus that lacks the glycine residue at the corresponding position (Supplementary Fig. S7).
503 However, the glycine residue is present in both floral activators and floral inhibitors of the FT-like
504 family, so its precise function in terms of floral regulation remains unclear. Additional amino acid
505 residues that are necessary for the regulatory activity of FT proteins have been described (Hanzawa
506 *et al.*, 2005; Ahn *et al.*, 2006; Ho and Weigel, 2014) and it seems likely that the presence of all these
507 conserved residues is required for the correct function of FT-like floral activators. However, further
508 studies are needed to understand in detail the role of the C-terminus of FT in flower development.

509 MM plants can flower under SD conditions, indicating that the high levels of mRNA encoding the
510 strong activator NtFT4 and the weak activator $NtFT5_{MM}$ under SD conditions are sufficient to induce
511 flowering, whereas the low levels of both transcripts under LD conditions are not (Fig. 1I,J). Only the
512 strong overexpression of $NtFT5_{MM}$ can overcome the non-flowering phenotype in SR1Δ*NtFT5* plants
513 (Fig. 3). However, even strong overexpression can only complement the non-flowering phenotype to
514 a certain extent, given that the transgenic 35S:$NtFT5_{MM}$//SR1Δ*NtFT5* plants still induce flower
515 development at a later time point compared to the SR1 vector control. Under SD conditions, the MM
516 plants flowered one week later than the day-neutral cultivar Hicks (Fig. 1). RNA interference (RNAi)
517 experiments in tobacco SR1 plants have shown that the silencing of *NtFT4* or *NtFT5* can delay
518 flowering, but the effect was stronger for *NtFT5* (Beinecke *et al.*, 2018). This suggests that NtFT5 has
519 a stronger effect than NtFT4 in flower development and explains the delayed flowering phenotype of
520 cultivar MM compared to day-neutral cultivar Hicks under SD conditions, given that the latter still
521 produces a functional NtFT5 protein.
522 Taken together, our results demonstrate that $NtFT5_{MM}$ acts as a weak floral activator even when
523 strongly overexpressed, which may reflect its lower binding affinity for NtFD. Thus, a possible model
524 for the MM phenotype is that, under LD conditions, the typical levels of $NtFT5_{MM}$ mRNA are
525 insufficient for floral induction, but under SD conditions floral induction in MM plants is facilitated by
526 the high levels of *NtFT4* mRNA, resulting in the switch from vegetative to reproductive growth. Thus,
527 our results provide insight into the SD-specific flowering behavior of MM, a tobacco cultivar that was
528 instrumental in the discovery of photoperiodism and was first described a century ago.

529 **Supplementary data**

530 **Fig. S1.** Detection of *NtFT7* in tobacco (*N. tabacum*) cultivars Maryland Mammoth (MM), Hicks and
531 SR1, and *N. sylvestris*.
532 **Fig. S2.** Phenotypic analyses of SR1ΔNtFT5 and MM plants expressing *NtFT5* or $NtFT5_{MM}$ under
533 control of the endogenous promoter P-$NtFT5_{2.6kb}$.
534 **Fig. S3.** BiFC analysis of $NtFT5_{R61G}$, $NtFT5_{R129A}$, $NtFT5_{FNC*}$ and AtFT with NtFD1 as well as NtFD3 and
535 NtFD4 with $NtFT5_{MM}$, NtFT5, $NtFT5_{FN*}$ and AtFT.
536 **Fig. S4.** Western blot analysis of BiFC experiments with different mRFP-FT fusion proteins and NtFD1.
537 **Fig. S5.** Multicolor BiFC assay.
538 **Figure S6.** Functional characterization of $NtFT5_{MM\ W170G}$ and $NtFT5_{G170W}$ mutants.
539 **Figure S7.** Amino acid sequence alignment of FT-like and TFL-like proteins.
540 **Table S1.** List of oligonucleotides used in this study.
541 **Table S2.** Geno- and phenotype of F_2 individuals.
542 **Methods S1.** Cloning procedures for BiFC.

543 **Acknowledgements**

544 We acknowledge the technical support of Michael Lahme, Christiane Fischer, Heike Hinte, Dewi
545 Hadisoetanto, Sai Aparna Nagarajan, Sascha Ahrens and Andreas Wagner.

546 **Author contributions**

547 LG, AK, DP, GAN: conceptualization, project administration and supervision; LG, MMZ, AK, AS, JM:
548 investigation; DRW: formal analysis; LG, MMZ: visualization; LG, MMZ, AK, RMT, GAN: writing

549 **Conflicts of interest**

550 The authors declare no conflict of interest.

551 **Funding**

552 This work was partially financed by grants from the Fraunhofer Society.

553 **Data availability**

554 All data supporting the findings of this study are available within the manuscript and its
555 supplementary materials.

References

Abe M, Kobayashi Y, Yamamoto S, Daimon Y, Yamaguchi A, Ikeda Y, Ichinoki H, Notaguchi M, Goto K and Araki T. 2005. FD, a bZIP Protein Mediating Signals from the Floral Pathway Integrator FT at the Shoot Apex. Science 309, 1052–1056.

Abelenda JA, Cruz-Oró E, Franco-Zorrilla JM, Prat S. 2016. Potato StCONSTANS-like1 Suppresses Storage Organ Formation by Directly Activating the FT-like StSP5G Repressor. Current Biology 26, 872–881.

Ahn JH, Miller D, Winter VJ, Banfield MJ, Lee JH, Yoo SY, Henz SR, Brady RL and Weigel D. 2006. A divergent external loop confers antagonistic activity on floral regulators FT and TFL1. EMBO Journal, 25: 605–614.

Amasino RM. 2013. My favourite flowering image: Maryland Mammoth tobacco. Journal of Experimental Botany 64, 5817–5818.

Banfield MJ, Barker JJ, Perry C and Brady RL. 1998. Function from structure? The crystal structure of human phosphatidylethanolamine-binding protein suggests a role in membrane signal transduction. Structure, 6: 1245–1254.

Beinecke FA, Grundmann L, Wiedmann DR, Schmidt FJ, Caesar AS, Zimmermann M, Lahme M, Twyman RM, Prüfer D and Noll GA. 2018. The FT/FD-dependent initiation of flowering under long-day conditions in the day-neutral species Nicotiana tabacum originates from the facultative short-day ancestor Nicotiana tomentosiformis. Plant Journal, 96: 329–342.

Bevan M. 1984. Binary Agrobacterium vectors for plant transformation. Nucleic Acids Research, 12: 8711–8721.

Bradley D, Carpenter R, Copsey L, Vincent C, Rothstein S and Coen E. 1996. Control of inflorescence architecture in Antirrhinum. Nature, 379: 791–797.

Cao K, Cui L, Zhou X, Ye L, Zou Z and Deng S. 2015. Four Tomato FLOWERING LOCUS T-Like Proteins Act Antagonistically to Regulate Floral Initiation. Frontiers in Plant Science, 6.

Collani S, Neumann M, Yant L, Schmid M. 2019. FT Modulates Genome-Wide DNA-Binding of the bZIP Transcription Factor FD. Plant Physiology 180, 367–380.

Corbesier L, Vincent C and Jang S 2007. FT Protein Movement Contributes to Long-Distance Signaling in Floral Induction of Arabidopsis. Science, 316: 1030–1033.

Garner WW and Allard HA. 1920. Effect of the relative length of day and night and other factors of the environment on growth and reproduction in plants. Journal of Agricultural Research, 18: 553–606.

Hamilton CM, Frary A, Lewis C and Tanksley SD. 1996. Stable transfer of intact high molecular weight DNA into plant chromosomes. PNAS USA, 93: 9975–9979.

Hanzawa Y, Money T and Bradley D. 2005. A single amino acid converts a repressor to an activator

of flowering. PNAS USA., 102: 7748–7753.

Harig L, Beinecke FA, Oltmanns J, Muth J, Müller O, Rüping B, Twyman RM, Fischer R, Prüfer D and Noll GA. 2012. Proteins from the FLOWERING LOCUS T-like subclade of the PEBP family act antagonistically to regulate floral initiation in tobacco. Plant Journal, 72: 908–921.

Ho WWH, Weigel D. 2014. Structural features determining flower-promoting activity of Arabidopsis FLOWERING LOCUS T. The Plant Cell 26, 552–564.

Hoekema A, Hirsch PR, Hooykaas PJJ and Schilperoort RA. 1983. A binary plant vector strategy based on separation of vir- and T-region of the Agrobacterium tumefaciens Ti-plasmid. Nature, 303: 179–180.

Horsch RB, Fry JE, Hoffmann NL, Eichholtz D, Rogers SG and Fraley RT. 1985. A Simple and General Method for Transferring Genes into Plants. Science, 227: 1229–1231.

Kardailsky I, Shukla VK, Ahn JH, Dagenais N, Christensen SK, Nguyen JT, Chory J, Harrison MJ and Weigel D. 1999. Activation Tagging of the Floral Inducer FT. Science, 286: 1962–1965.

Karlgren A, Gyllenstrand N, Källman T, Sundström JF, Moore D, Lascoux M and Lagercrantz U. 2011. Evolution of the PEBP gene family in plants: functional diversification in seed plant evolution. Plant Physiology, 156: 1967–1977.

Kim S-J, Yoo SJ, Hong SM, Ahn JH, Moon S and Jung HS. 2016. Post-Translational Regulation of FLOWERING LOCUS T Protein in Arabidopsis. Molecular Plant, 9: 308–311.

Kobayashi Y, Kaya H, Goto K, Iwabuchi M and Araki T. 1999. A Pair of Related Genes with Antagonistic Roles in Mediating Flowering Signals. Science, 286: 1960–1962.

Koornneef M, Hanhart CJ and van der Veen JH. 1991. A genetic and physiological analysis of late flowering mutants in Arabidopsis thaliana. Molecular and General Genetics, 229: 57–66.

Lifschitz E, Eviatar T, Rozman A, Shalit A, Goldshmidt A, Amsellem Z, Alvarez JP and Eshed Y. 2006. The tomato *FT* ortholog triggers systemic signals that regulate growth and flowering and substitute for diverse environmental stimuli. PNAS USA, 103: 6398–6403.

Livak KJ and Schmittgen TD. 2001. Analysis of Relative Gene Expression Data Using Real-Time Quantitative PCR and the $2^{-\Delta\Delta C_T}$ Method. Methods, 25: 402–408.

Molinero-Rosales N, Latorre A, Jamilena M and Lozano R. 2004. SINGLE FLOWER TRUSS regulates the transition and maintenance of flowering in tomato. Planta, 218: 427–434.

Müller B, Noll GA, Ernst AM, Rüping B, Groscurth S, Twyman RM, Kawchuk LM and Prüfer D. 2010. Recombinant artificial forisomes provide ample quantities of smart biomaterials for use in technical devices. Applied Microbiology and Biotechnology, 88: 689–698.

Murashige T and Skoog F. 1962. A Revised Medium for Rapid Growth and Bio Assays with Tobacco Tissue Cultures. Physiologia Plantarum, 15: 473–497.

Pin PA, Benlloch R, Bonnet D, Wremerth-Weich E, Kraft T, Gielen JJL and Nilsson O. 2010. An Antagonistic Pair of *FT* Homologs Mediates the Control of Flowering Time in Sugar Beet. Science, 330: 1397–1400.

Pnueli L, Gutfinger T, Hareven D *et al.* 2001. Tomato SP-interacting proteins define a conserved signaling system that regulates shoot architecture and flowering. The Plant Cell 13, 2687–2702.

Post J, Eisenreich W, Huber C, Twyman RM, Prüfer D, Schulze Gronover C. 2014. Establishment of an ex vivo laticifer cell suspension culture from *Taraxacum brevicorniculatum* as a production system for cis-isoprene. Journal of Molecular Catalysis B: Enzymatic 103, 85–93.

Schmidt FJ, Zimmermann MM, Wiedmann DR, Lichtenauer S, Grundmann L, Muth J, Twyman RM, Prüfer D, and Noll GA. 2020.. The Major Floral Promoter NtFT5 in Tobacco Nicotiana tabacum. Is a Promising Target for Crop Improvement. Frontiers in Plant Sciences, 10: 1–16.

Schmidt GW and Delaney SK. 2010. Stable internal reference genes for normalization of real-time RT-PCR in tobacco *Nicotiana tabacum*. during development and abiotic stress. Molecular Genetics and Genomics, 283: 233–241.

Schoentgen F and Jollès P. 1995. From structure to function: possible biological roles of a new widespread protein family binding hydrophobic ligands and displaying a nucleotide binding site. FEBS Letter, 369: 22–26.

Smith SM, McDaniel CN. 1992. The Maryland mammoth allele and rooting both perturb the fate of florally determined apices in *Nicotiana tabacum*. Developmental Biology 153, 176–184.

Tamaki S, Matsuo S, Wong HL, Yokoi S and Shimamoto K. 2007. Hd3a Protein Is a Mobile Flowering Signal in Rice. Science, 316: 1033–1036.

Taoka K, Ohki I, Tsuji H *et al.* 2011. 14-3-3 proteins act as intracellular receptors for rice Hd3a florigen. Nature, 476: 332–335.

Töpfer R, Matzeit V, Gronenborn B, Schell J and Steinbiss H-H. 1987. A set of plant expression vectors for transcriptional and translational fusions. Nucleic Acids Research, 15: 5890.

Turck F, Fornara F, and Coupland G. 2008. Regulation and Identity of Florigen: FLOWERING LOCUS T Moves Center Stage. Annual Review of Plant Biology 59: 573-594

Walter M, Chaban C, Schütze K, Batistic O, Weckermann K, Näke C, Blazevic D, Grafen C, Schumacher K, Oecking C, Harter K and Kudla J. 2004. Visualization of protein interactions in living plant cells using bimolecular fluorescence complementation. Plant Journal 40: 428–438.

Wang G, Li Y, Gao J, Zhao M, Xia Q, Wang P, Wu L and Gao Y. 2018. Isolation and functional characterization of a novel FLOWERING LOCUS T homolog *NtFT5*. in *Nicotiana tabacum*. Journal of Plant Physiology, 231: 393–401.

Wickland DP and Hanzawa Y. 2015. The *FLOWERING LOCUS T/TERMINAL* FLOWER 1 Gene Family: Functional Evolution and Molecular Mechanisms. Molecular Plant, 8: 983–997.

Wigge PA, Kim MC, Jaeger KE, Busch W, Schmid M, Lohmann JU and Weigel D. 2005. Integration of Spatial and Temporal Information During Floral Induction in *Arabidopsis*. Science, 309: 1056–1059.

Zuo X, Wang S, Xiang W *et al.* 2021. Genome-wide identification of the 14-3-3 gene family and its participation in floral transition by interacting with TFL1/FT in apple. BMC genomics 22, 41.

Figures and figure legends

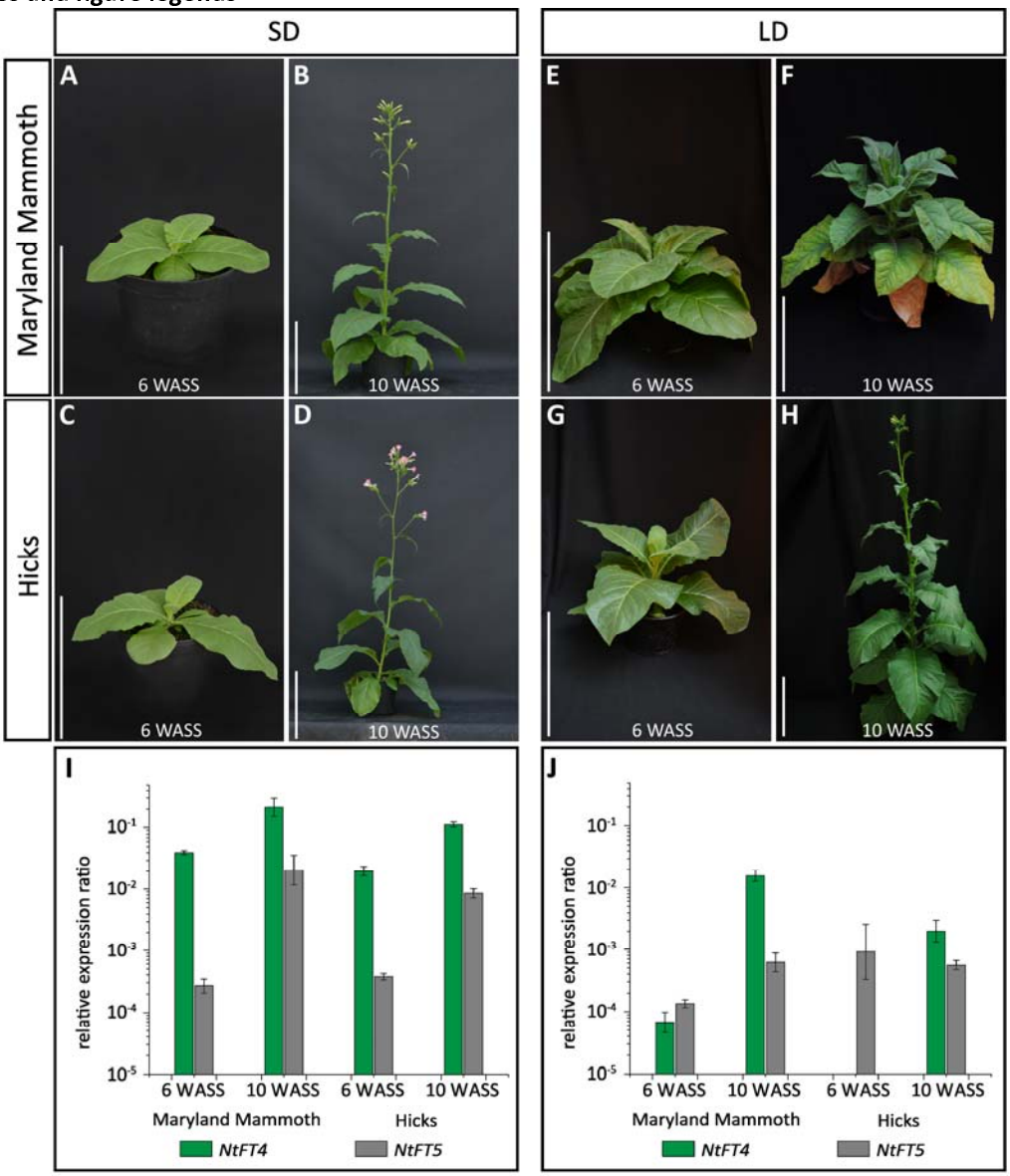

Fig. 1. Phenotype and *NtFT4/NtFT5* gene expression in tobacco cultivars Maryland Mammoth (MM) and Hicks under short-day (SD) and long-day (LD) conditions.

(A–D) Under SD conditions, flower development was observed both for (A,B) cv. MM and (C,D) cv. Hicks.

(E–H) Under LD conditions, (E,F) no flower development was observed in cv. MM, but (G,H) flowers were produced by cv. Hicks. Pictures were taken 6 and 10 weeks after seed sowing (WASS). Scale bars = 30 cm.

(I,J) *NtFT4* and *NtFT5* expression was analyzed by qPCR in three biological replicates per time point. Each biological replicate comprised pooled medial leaf tissue of three individual plants. Values were normalized to the reference gene *NtEF-1α*. Error bars represent the standard error of the mean of three biological replicates. *NtFT4* is predominantly expressed under SD conditions with rising mRNA levels during the reproductive phase in both cultivars. Under LD conditions, *NtFT4* mRNA levels were low (MM) or not detectable (Hicks) 6 WASS but increased in both cultivars 10 WASS. *NtFT5* expression increased with the initiation of floral development in both cultivars under SD conditions. Under LD conditions, the expression of *NtFT5* was higher in Hicks than in MM 6 WASS, but mRNA levels were similar in both cultivars 10 WASS.

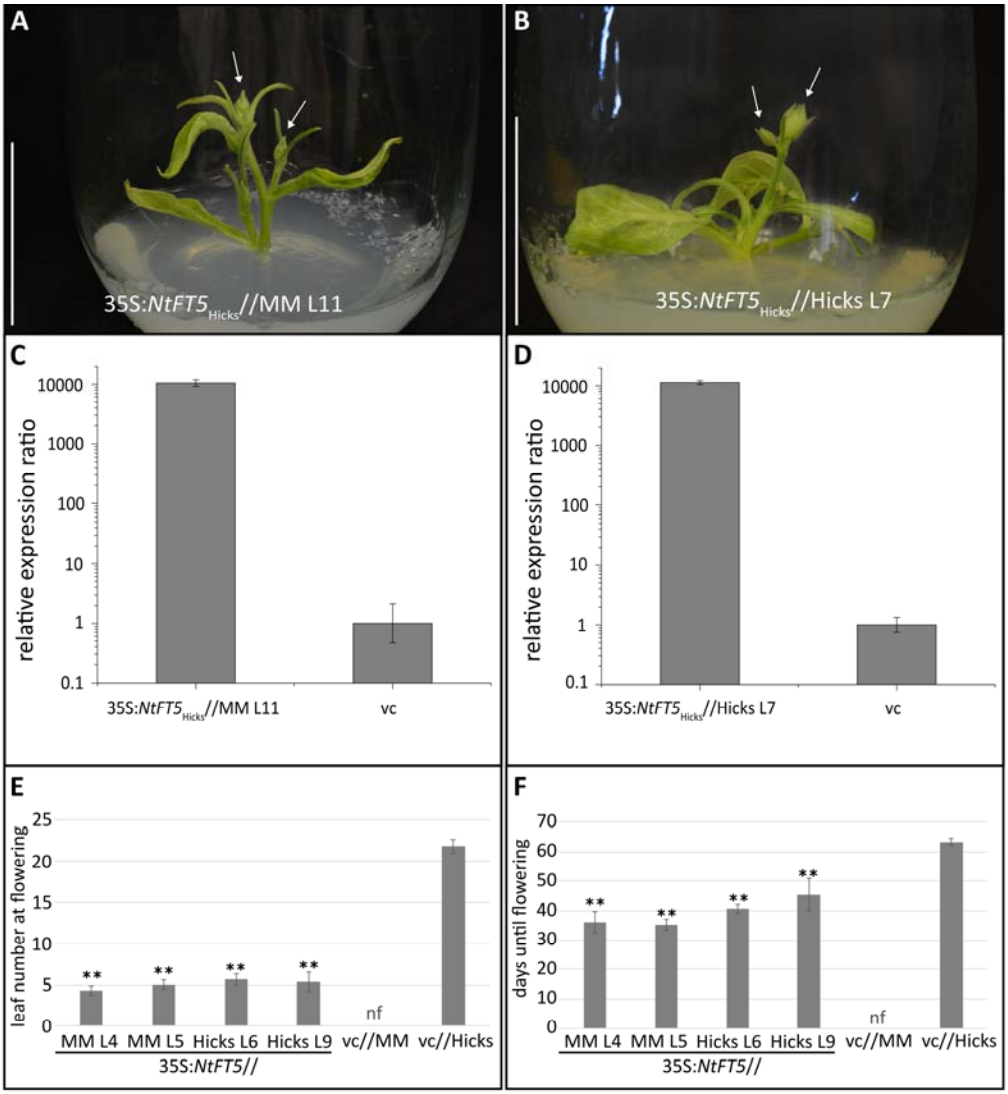

Fig. 2. Overexpression of *NtFT5*$_{\text{Hicks}}$ leads to early flowering in tobacco cultivars Maryland Mammoth (MM) and Hicks.

(A,B) Constitutive overexpression of *NtFT5*$_{\text{Hicks}}$ causes early flowering in tobacco (A) cv. MM and (B) cv. Hicks. Pictures were taken in tissue culture. Arrows indicate the formation of buds. Scale bars = 5 cm.

(C,D) *NtFT5*$_{\text{Hicks}}$ expression was analyzed by qPCR using samples isolated from entire plants harvested at the tissue culture stage. Values were normalized to the reference gene *NtEF-1α*. Expression in the vector control (vc) was set to 1 and error bars represent the combined standard deviation of target and reference gene technical replicates. *NtFT5*$_{\text{Hicks}}$ mRNA levels were >10^4-fold higher in MM L11 and Hicks L7 transgenic plants than the corresponding vector controls.

(E) In T_1 generation, all plants were grown in the greenhouse under LD conditions. The total number of leaves was determined when the first flower had opened. All lines of plants overexpressing *NtFT5* produced fewer leaves than the Hicks vector control.

(F) The number of days until flowering was defined as the period between seed sowing and the day the first flower opened. Strong overexpression of *NtFT5* in MM and Hicks plants resulted in profound early flowering phenotypes compared to the Hicks and the non-flowering (nf) MM vector controls under LD conditions.

(E,F) Mean values are shown for two 35S:*NtFT5*//MM lines (L4 and L5, n = 10), two 35S:*NtFT5*//Hicks lines (L6 n = 10, and L9, n = 9) and one vector control line for MM and Hicks (n = 10), respectively, with error bars representing ± 95% confidence intervals. Normal distribution was confirmed by applying the Kolmogorov-Smirnov test. Statistical significance was determined using a pairwise Welch's *t*-test with Bonferroni-Holm correction (**$P < 0.01$). nf = non-flowering

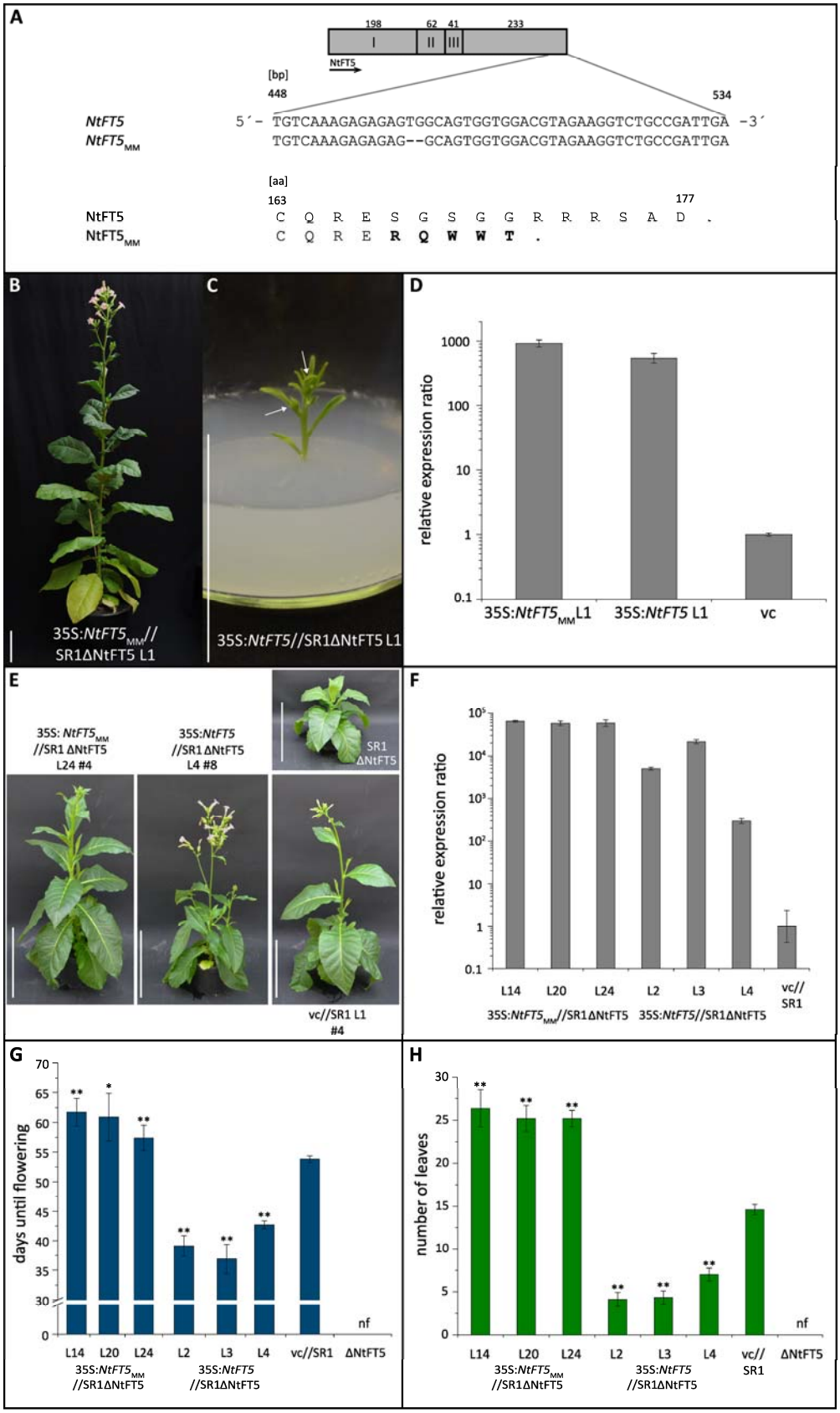

Fig. 3. Phenotypic and molecular analysis of *NtFT5* and *NtFT5*$_{MM}$ overexpression in SR1Δ*NtFT5* plants.

(A) Exon structure of *NtFT5* and sequence alignment of the 3′ end of the coding sequence showing a 2-bp deletion 29 bp upstream of the typical stop codon in $NtFT5_{MM}$ resulting in a truncated amino acid sequence.
(B) Constitutive overexpression of $NtFT5_{MM}$ in SR1Δ*NtFT5* plants led to flower development in the greenhouse when the plants reached approximately 1.2 m in height. Scale bar = 10 cm.
(C) In contrast, *NtFT5* overexpression in SR1Δ*NtFT5* plants caused a profound early flowering phenotype in tissue culture. Arrows indicate the formation of buds. Scale bar = 10 cm.
(D) $NtFT5_{MM}$ and *NtFT5* expression was analyzed by qPCR using samples isolated from leaf material ($NtFT5_{MM}$) and the whole plant shoot for *NtFT5* and vector control (vc), both harvested in tissue culture. The values were normalized to the reference gene *NtEF-1α*. Expression in the vector control was set to 1 and error bars represent the combined standard deviation of the target and reference gene technical replicates. $NtFT5_{MM}$ mRNA (920-fold higher than vector control) and *NtFT5* mRNA (540-fold higher than vector control) levels strongly increased in both transgenic lines.
(E) Constitutive overexpression of $NtFT5_{MM}$ in the non-flowering SR1Δ*NtFT5* background caused delayed flowering compared to the wild-type SR1 vector control (vc) under LD conditions (T_1 generation), indicating only partial complementation, whereas overexpression of *NtFT5* induced early flowering in transgenic plants. Scale bars = 30 cm.
(F) $NtFT5_{MM}$ and *NtFT5* expression was analyzed by qPCR using samples isolated from five pooled seedlings. The values were normalized to the reference gene *NtEF-1α*. Expression in the vector control was set to 1 and error bars represent the combined standard deviation of the target and reference gene technical replicates. The levels of $NtFT5_{MM}$ mRNA were higher in all lines compared to the vector control, ranging from 58,000-fold (L20 and L24) to 64,000-fold (L14). *NtFT5* transcript levels ranged from 300-fold (L4) to 22,000-fold (L3) higher than the vector control.
(G) The number of days until flowering was defined as the period between seed sowing and the day the first flower opened. Strong overexpression of $NtFT5_{MM}$ in SR1Δ*NtFT5* plants resulted in delayed flowering in all transgenic lines compared to the SR1 vector control. Plants overexpressing *NtFT5* showed profound early flowering phenotypes compared the SR1 vector control.
(H) The total number of leaves was determined when the first flower had opened. All lines of SR1Δ*NtFT5* plants overexpressing $NtFT5_{MM}$ produced more leaves and all lines overexpressing *NtFT5* produced fewer leaves than the SR1 vector control.
(G,H) Mean values are shown for three 35S:$NtFT5_{MM}$//SR1Δ*NtFT5* lines (L14 and L24, n = 10; L20, n = 8), three 35S:$NtFT5_{MM}$//SR1Δ*NtFT5* lines (L2 and L3, n = 9; L4, n = 10) and one vector control line (n = 10) with error bars representing ± 95% confidence intervals. Normal distribution was confirmed by applying the Kolmogorov-Smirnov test. Statistical significance was determined using a pairwise Welch's *t*-test with Bonferroni-Holm correction (**$P < 0.01$; *$P < 0.05$). nf = non-flowering

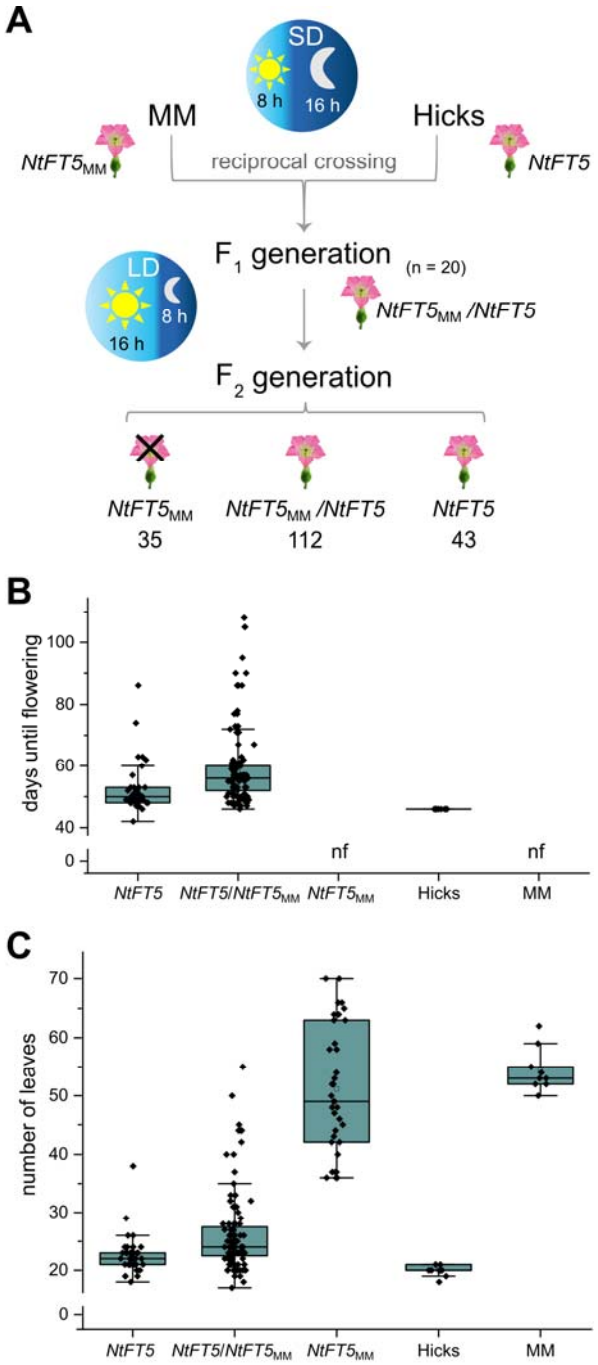

Fig. 4. Reciprocal crossings of the cultivars Hicks and MM.

(A) Experimental workflow of the crossing experiment. Flowering MM and Hicks plants were crossed reciprocally. In the F_1 generation (n = 20) all plants flowered and showed a heterozygous NtFT5/NtFT5$_{MM}$ genotype. Detailed phenotyping of non-flowering homozygous NtFT5$_{MM}$ plants and flowering NtFT5 and NtFT5/NtFT5$_{MM}$ plants was finally carried out in the F_2 generation.

(B) The number of days until flowering was defined as the period between seed sowing and the day the first flower opened. The presence of two functional NtFT5 alleles in F_2 individuals mediated a normal flowering phenotype, while the presence of NtFT5/NtFT5$_{MM}$ alleles mediated a delayed flowering phenotype. All F_2 individuals with two NtFT5$_{MM}$ alleles did not flower like the MM plants (nf = non-flowering).

(C) The total number of leaves was determined when the first flower had opened (in case of non-flowering NtFT5$_{MM}$ and MM plants at the end of the experiment after 120 days).

(B,C) In the boxplots, center line = median, square = mean, box limits = upper and lower quartiles, whiskers = 1.5× interquartile range, and diamonds = individual data points.

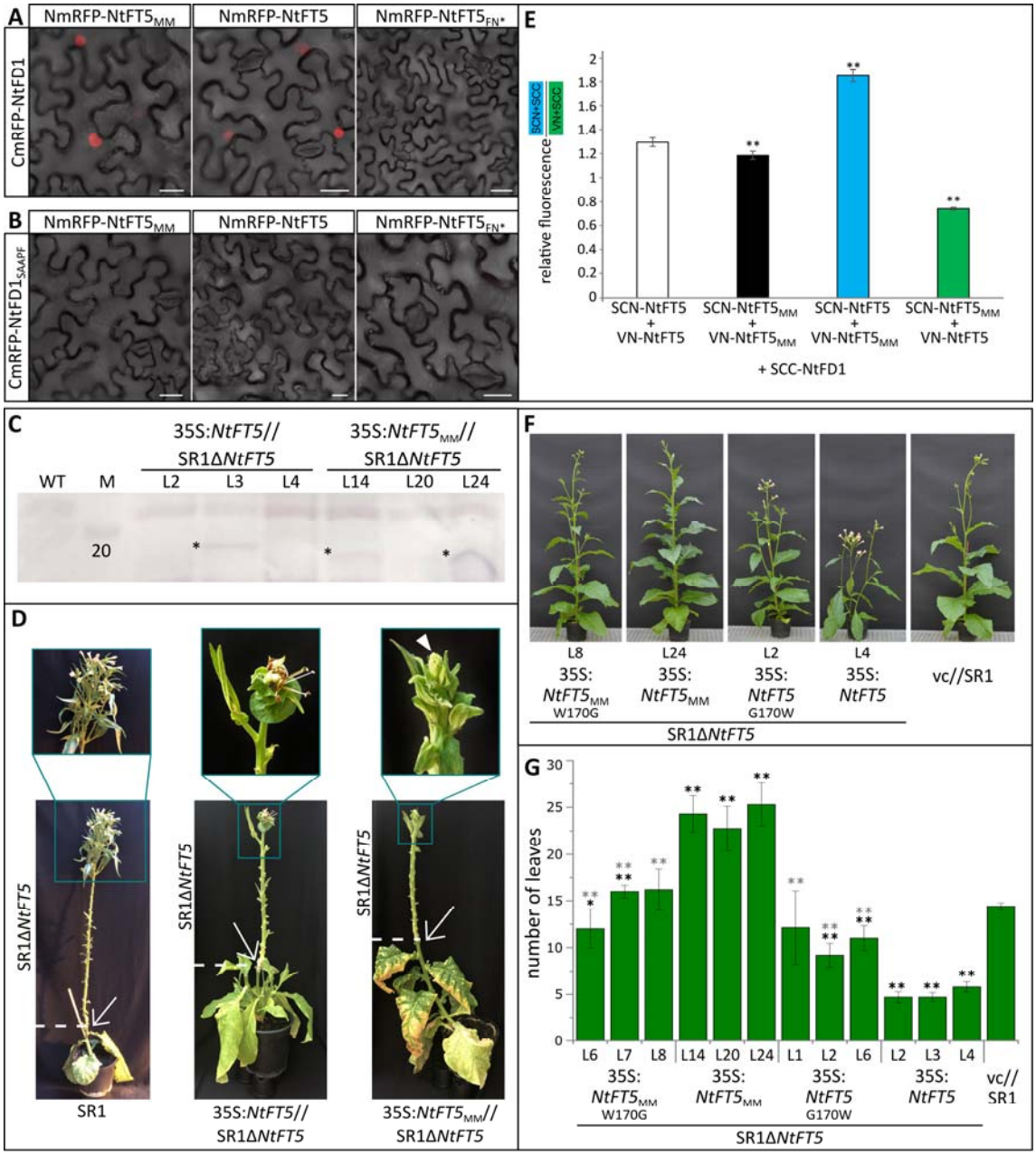

Fig. 5. Functional characterization of NtFT5$_{MM}$ and NtFT5.

(A,B) BiFC analysis revealed that NtFD1 (A) interacts with NtFT5$_{MM}$ and NtFT5 in *N. benthamiana* leaf epidermal cells, whereas NtFD1$_{SAAPF}$ (B) does not interact with the tobacco FTs; 35S:*CmRFP-NtFD1* or 35S:*CmRFP-NtFD1*$_{SAAPF}$ was co-expressed with 35S:*NmRFP* fusions of *NtFT5*$_{MM}$, *NtFT5* and *NtFT5*$_{FN*}$. Scale bars = 25 µm.

(C) Detection of NtFT5 and NtFT5$_{MM}$ proteins by western blotting. We loaded 50 mg of protein extracted from seedlings in each lane and detected the NtFT protein (*) with an AtFT-specific primary antibody and an alkaline phosphatase-labeled secondary antibody. The Precision Plus Protein standards were used as size markers (M).

(D) Grafting experiments confirming that the NtFT5 and NtFT5$_{MM}$ proteins are transported from wild-type (WT), 35S:*NtFT5* and 35S:*NtFT5*$_{MM}$ stock to the SAM to induce flower-like structures on SR1Δ*NtFT5* scions. Pictures were taken when scions flowered. Emerging leaves on the scion and axillary shoots on the stock were removed regularly to enhance the source–sink gradient.

(E) In mcBiFC assays, NtFD1 preferentially associated with NtFT5 rather than NtFT5$_{MM}$. T-DNAs carrying two CaMV 35S cassettes encoding combinations of SCN and VN fusion proteins were introduced into *N. benthamiana* leaf epidermal cells together with a separate T-DNA containing a 35S:*SCC-NtFD1* construct.

SCN+SCC and VN+SCC fluorescence was measured in the nuclei. Values represent the SCN+SCC signal divided by the VN+SCC signal. Error bars indicate 95% confidence intervals for means. Sample sizes (left to right): 428, 341, 535, 542. SCN, N-terminal part of S(CFP)3A; VN, N-terminal part of Venus; SCC, C-terminal part of S(CFP)3A. Statistical significance was determined using a pairwise Welch's t-test with Bonferroni-Holm correction (**$P < 0.01$).

(F) Replacing the tryptophan residue in NtFT5$_{MM}$ with glycine in transgenic 35S:*NtFT5*$_{MM\ W170G}$//SR1Δ*NtFT5* lines resulted in a WT-like flowering phenotype, whereas mutating the glycine residue to tryptophan in transgenic 35S:*NtFT5*$_{G170W}$//SR1Δ*NtFT5* lines abolished the profound early flowering phenotype under LD conditions (T_1 generation). One line each is shown as an example.

(G) The number of leaves was determined when the first flower opened. All SR1Δ*NtFT5* lines overexpressing *NtFT5*$_{MM}$ produced more leaves and all lines overexpressing *NtFT5* produced fewer leaves than the SR1 vector control. The 35S:*NtFT5*$_{G170W}$//SR1Δ*NtFT5* lines produced more leaves and the 35S:*NtFT5*$_{MM\ G170W}$//SR1Δ*NtFT5* lines produced fewer leaves than the corresponding 35S:*NtFT5*$_{(MM)}$//SR1Δ*NtFT5* lines. Mean values are shown for three 35S:*NtFT5*$_{MM}$//SR1Δ*NtFT5* lines (L14 and L24, n = 10; L20, n = 8), three 35S:*NtFT5*$_{MM}$//SR1Δ*NtFT5* lines (L2, L3 and L4, n = 10), three 35S:*NtFT5*$_{MM\ W170G}$//SR1Δ*NtFT5* lines (L6, L7 and L8, n = 10), three 35S:*NtFT5*$_{G170W}$//SR1Δ*NtFT5* lines (L1, n = 8; L2 n = 10; L6, n = 6) and one vector control line (n = 10) with error bars representing ± 95% confidence intervals. Normal distribution was confirmed by applying the Kolmogorov-Smirnov test. Statistical significance was determined using a pairwise Welch's *t*-test with Bonferroni-Holm correction (**$P < 0.01$; *$P < 0.05$; black = significant compared to vc; gray = significant compared to corresponding native construct).